Excited-State Trions in Monolayer WS_2

Ashish Arora,[1*,†] Thorsten Deilmann,[2,†] Till Reichenauer,[1] Johannes Kern,[1] Steffen Michaelis de Vasconcellos,[1] Michael Rohlfing,[2] and Rudolf Bratschitsch[1]

[1]*Institute of Physics and Center for Nanotechnology, University of Münster, Wilhelm-Klemm-Straße 10, 48149 Münster, Germany*

[2]*Institute of Solid State Theory, Wilhelm-Klemm-Straße 10, University of Münster, 48149 Münster, Germany*

(Received 8 March 2019; published 17 October 2019)

We discover an excited bound three-particle state, the 2*s* trion, appearing energetically below the 2*s* exciton in monolayer WS_2, using absorption spectroscopy and *ab initio* GW and Bethe-Salpeter equation calculations. The measured binding energy of the 2*s* trion (22 meV) is smaller compared to the 1*s* intravalley and intervalley trions (37 and 31 meV). With increasing temperature, the 1*s* and 2*s* trions transfer their oscillator strengths to the respective neutral excitons, establishing an optical fingerprint of trion-exciton resonance pairs. Our discovery underlines the importance of trions for the entire excitation spectrum of two-dimensional semiconductors.

DOI: 10.1103/PhysRevLett.123.167401

Three-particle bound states called trions have been extensively used to study many-body physics in semiconductors [1]. Since their first prediction in 1958 [2] it took until the 1970s to confirm their existence, partially due to their low binding energies (E_b^T) below 1 meV for typical bulk semiconductors [3,4]. The first signatures of trions were observed in bulk Ge [3], Si [4], and CuCl [5]. Following the predictions of higher binding energies in nanostructures providing carrier confinement [6], trions were experimentally observed in CdTe quantum wells ($E_b^T = 2.65$ meV) [7], in GaAs quantum wells ($E_b^T = 2$ meV) [8], in an ensemble of self-assembled InAs quantum dots ($E_b^T = 10$ to 20 meV) [9], and later on, in carbon nanotubes ($E_b^T = 130$ meV) [10].

Strikingly, with the advent of monolayers of transition metal dichalcogenides (TMDCs) such as MoS_2, strongly bound neutral excitons (E_b^X up to 0.8 eV) [11–13] and charged excitons (trions) have been observed in these true 2D systems. Trions are found energetically below the neutral *A* exciton state with binding energies on the order of 30 meV [14]. Such strong Coulomb effects provide an excellent platform to investigate many-body physics such as excited (Rydberg) exciton states [11,12,15], biexcitons [16–21], and five-particle complexes [17–21] in TMDC monolayers.

The Coulomb interaction between electrons and holes is strongly influenced by the dielectric screening that is drastically reduced in TMDC monolayers when compared to conventional III-V or II-VI heterostructures. This leads to strong deviations from the 2D hydrogenic Rydberg model of excitons [11,12]. It sparked widespread interest in calculating the interaction of light with excitons and trions in semiconducting monolayers using *ab initio* theory [22–24], and other approaches involving the Rytova-Keldysh potential [11,25], the Berry phase [26,27], and massive 2D Dirac excitons [28]. Recently, another emerging interpretation considers trions as excitations, where excitons reside in a Fermi sea of excess charges ("exciton-polarons") [29–31]. Although there are significant advancements in understanding the neutral exciton spectra [11,12,22,25–28,32,33], efforts to calculate the optical excitations of trions are limited [25,32–36]. A parameter-based study has theoretically proposed the possibility of excited-state trions [34]. In contrast, the simplest three-particle system of one positive and two negative charges, the H^- ion, does not have bound excited states beyond the ground state [37]. This poses the basic question if the 2*s* exciton of a TMDC monolayer can be accompanied by a 2*s* trion or not. Here, we perform absorption measurements on WS_2 monolayers encapsulated in hBN as a function of temperature. Supported by *ab initio* calculations employing the GW approximation and the Bethe-Salpeter equation (BSE), we discover the excited state of a trion.

Figure 1(a) shows the absorption spectrum (orange line) of an hBN-encapsulated WS_2 monolayer on sapphire substrate measured in a wide energy range at cryogenic temperature ($T = 5$ K) [38]. The encapsulation with thin sheets of hBN (4 nm top and 23 nm bottom) is known to narrow excitonic lines in the optical spectra approaching the homogeneous limit [55–57]. Another significant effect of hBN encapsulation is an additional dielectric screening resulting in redshifted lines, as well as a reduced quasiparticle binding energies compared to TMDC monolayers in vacuum. At low energy, three prominent resonances are visible in absorption, which are shown in Fig. 1(b) together with a model (black line), where each resonance is represented by a Lorentzian [38]. Nearly Lorentzian line shapes of the three resonances are found and identified as

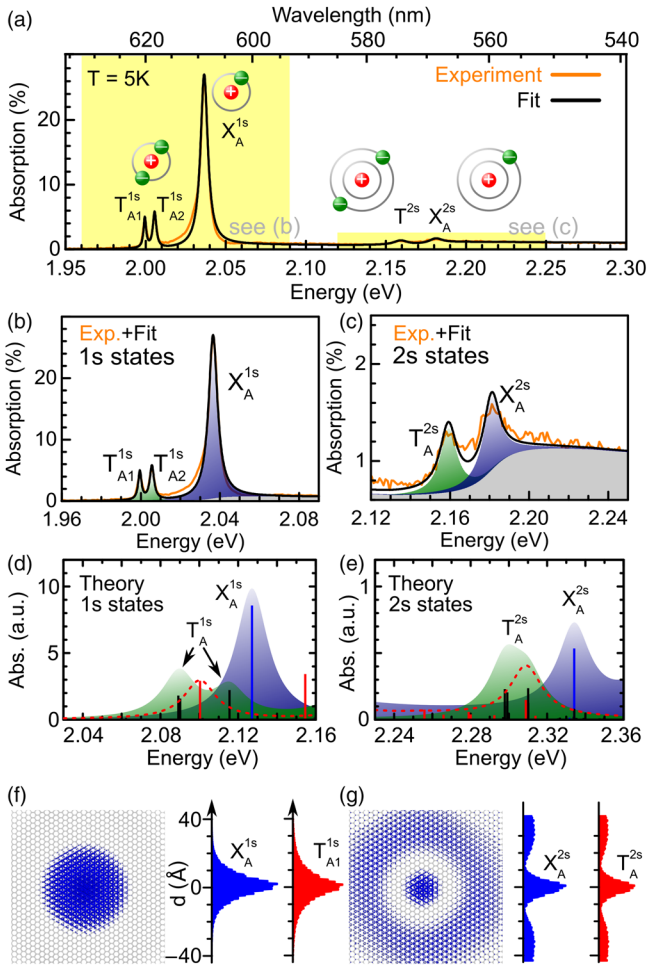

FIG. 1. (a) Optical absorption spectrum of a hBN-encapsulated WS_2 monolayer on sapphire substrate measured at a temperature $T = 5$ K (orange) along with the fitted curve (black, see Supplemental Material [38] for details). The ground ($n = 1$) state of the A exciton, X_A^{1s}, the intravalley and intervalley trions T_{A1}^{1s} and T_{A2}^{1s}, respectively, are clearly identified. Additionally, excited ($n = 2$) states of A excitations X_A^{2s} and T_A^{2s} are visible. (b) Experimental and fitted spectra for ($n = 1$) states, where shaded green and blue regions represent the contributions from trions and excitons, respectively. (c) Zoomed-in view highlighting ($n = 2$) excited state trions T_A^{2s} and excitons X_A^{2s} along with the fitted spectrum. (d),(e) Calculated optical absorption of neutral excitons (shaded blue) and positive (dashed-red line) and negative trions (shaded green). The bound excitations are labeled, while the unlabeled excitations (red or black bars) represent scattering states which are not fully converged (and thus excluded in the plotted curves). We use an artificial Lorentzian broadening with a width of 10 meV. Left panels of (f) and (g) display top views of the calculated probability distribution of the $1s$ [in (f)] and $2s$ [in (g)] exciton and trion states, as described in the text and Supplemental Material [38]. The right side represents cross-sectional views around the mid vertical of the spatial distribution displayed on the left.

the ground state ($n = 1$) A exciton (X_A^{1s} at 2.036 eV), the intravalley trion (T_{A1}^{1s} at 2.000 eV), and the intervalley trion (T_{A2}^{1s} at 2.006 eV). Intravalley and intervalley trions are denoted following Ref. [58]. The presence of two trion resonances suggests n-type doping of the WS_2 [33,58,59]; i.e., they are two negatively charged trions. The binding energies for the intravalley and intervalley trions, measured via their energy difference to the neutral exciton X_A^{1s} are 37 and 31 meV, respectively. The energetic separation of 6 meV between the two trions agrees well with 7 ± 0.5 meV of an earlier report on a hBN-encapsulated WS_2 monolayer [60]. All three features T_{A1}^{1s}, T_{A2}^{1s}, and X_A^{1s} have narrow full width at half maximum (FWHM) linewidths of 2.0, 2.6, and 5.5 meV, respectively. This result signifies the very good interfacial quality in our sample, with linewidths approaching the homogeneous limit [55–57]. The larger linewidth of the neutral exciton compared to the trions is possibly due to the presence of additional low-energy states for the neutral exciton to decay into (e.g., to the trions or to optically dark states [33]).

Our GW-BSE calculated absorption spectrum [Fig. 1(d)] for the low-energy spectral region reveals distinct resonances of the neutral X_A^{1s} exciton, as well as for several three-particle excitations. Our calculations include the effect of the hBN layers encapsulating the 1L WS_2 crystal [38]. In the case of negative doping, we find three different inter- and intravalley excitations. Assuming a hole in the K^+ valley, the two electrons may occupy the four conduction band states (two states in each K^+ and K^- valley) in three different ways [33,35]. Overall, the three excitations appear as two maxima in the spectrum due to the energetic proximity of the first two trions (solid-black vertical lines). The trion binding energy of the three negative trions T_{A1}^{1s}, T_{A2}^{1s}, and T_{A3}^{1s} is 37, 36, and 11 meV, respectively. Only one trion is present for positive doping (dashed-red line, binding energy of 27 meV) [33,35]. Considering the finite computational accuracy and experimental resolution, we find a good agreement between theory and experiment for the negative trions. The $1s$ character of the resonances is confirmed by calculating the exciton wave function. The electron is fixed in the center, and the probability of finding the hole at a different location is indicated in Fig. 1(f). We present the top view of the probability distribution for X_A^{1s} (left side), as well as a cross-sectional view through the center of the distribution for X_A^{1s} and T_{A1}^{1s}. A clear resemblance with the $1s$ orbital of an H atom confirms the character of these excitations.

Strikingly, in our experiment, we measure two prominent resonances at 2.159 and 2.181 eV at higher energies in the absorption spectrum [Fig. 1(a) and zoomed-in spectrum in Fig. 1(c), see Supplemental Material [38] for a discussion of the steplike features]. We identify them as the excited state trion (T_A^{2s}) and the corresponding $2s$ excitonic counterpart X_A^{2s}, respectively. The schematic representation of the excited states following Bohr's atomic model is depicted in Fig. 1(a), where the corresponding electrons are in the second shell. The binding energy of T_A^{2s}, measured as

the energy difference with regards to X_A^{2s}, is 22 meV, which is smaller than for the 1s trions. This is conceivable, since being an excited state, T_A^{2s} is more loosely bound when compared to the ground state T_A^{1s}. Similar to the two 1s trion lines, one could expect also more than one 2s trion feature. However, their energetic proximity and larger linewidth probably causes them to merge into the measured single broad feature with a FWHM linewidth of 10.3 meV. The GW-BSE calculated absorption spectrum in the corresponding spectral region is plotted in Fig. 1(e) for negative (shaded green) and positive (dashed-red line) trions. The negative 2s trions have calculated binding energies of 35, 34, and 24 meV, respectively, whereas only one positive trion is found with a binding energy of 25 meV. The calculated spatial distribution of 2s excitations is shown in Fig. 1(g). The presence of a node and the striking similarity to the distribution of the hydrogenic 2s state verifies the 2s nature of both calculated states. Trions corresponding to higher excited 3s, 4s, etc., excitons might be present as well, with decreasing binding energies with increasing state number. However, we did not resolve these $n \geq 3$ excited states in our experiment, possibly due to their feeble oscillator strengths and their proximity to the quasiparticle band gap [43].

A further piece of evidence concerning the character of the observed resonances, being the ground states (T_{A1}^{1s} and T_{A2}^{1s}) and excited state of the trion T_A^{2s}, is obtained from temperature-dependent measurements. Figure 2 presents absorption spectra around the 1s exciton and trion states of the hBN-encapsulated WS_2 monolayer as a function of temperature. The extracted transition energies, FWHM linewidths, and the oscillator strength parameters (integrated area under the fitted Lorentzian, proportional to the transition strength) from the fitted spectra in Fig. 2(a) are plotted in Figs. 2(b)–2(d), respectively. Several observations are evident. (i) All excitations (excitons and trions) experience an identical redshift with rising temperature. (ii) The linewidth of the X_A^{1s} excitation increases with temperature. Among the two 1s trions, the linewidth of T_{A2}^{1s} (high-energy trion) increases by a factor of 2, while the one of T_{A1}^{1s} (low-energy trion) almost stays unchanged until $T = 50$ K. (iii) The oscillator strength of the T_{A1}^{1s} and T_{A2}^{1s} decreases at higher temperatures, while the neutral exciton X_A^{1s} rises.

Some of these temperature-dependent effects have been observed and discussed before [61–66]. The redshift (i) has been reported previously [63,64] and can be explained by two simultaneous effects. First, the lattice expands and reduces the band gap and therefore the excitation energies [67]. Second, polaron effects can lead to much stronger redshifts [62]. Likewise, the enhanced phonon density, which is responsible for the polaron shift, also leads to observation (ii); i.e., it increases the T_A^{1s} and X_A^{1s} linewidths with increasing temperatures [65,66]. Because of the

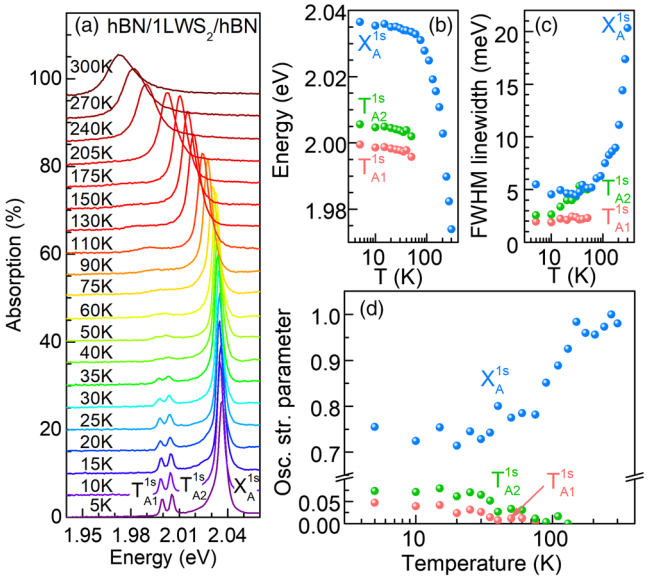

FIG. 2. (a) Absorption spectrum around the ($n = 1$) A exciton measured as a function of temperature ($T = 5$–300 K). The spectra are shifted along the y axis for clarity. The spectral line shapes are fitted as described in the text. The transition energies, FWHM linewidths, and oscillator strength parameters of the 1s intravalley (T_{A1}^{1s}) and intervalley (T_{A2}^{1s}) trions, and 1s exciton (X_A^{1s}) are plotted in (b), (c), and (d), respectively. Notably, in (d), both 1s trions lose oscillator strength, while the 1s exciton gains strength, as the temperature is increased.

different coupling strength to phonons and relative energetic alignments, the exact values are different. Finally, we come back to observation (iii), the transfer of oscillator strength from the T_{A1}^{1s} and T_{A2}^{1s} trions to their neutral exciton counterpart X_A^{1s} as the temperature is increased in Fig. 2. Earlier experiments on III-V and II-VI semiconductor quantum wells (e.g., based on ZnSe [68] and CdTe [69]) and on monolayer WSe_2 [63] showed that the oscillator strength from the 1s trion is transferred to the 1s exciton when the temperature of the sample is increased. As a result, the trion signal gradually disappears, while the neutral exciton becomes stronger. This effect is a well-known fingerprint of a T-X pair in a photoluminescence (PL) spectrum [46,63,68–70]. For an n-doped system (as our WS_2 monolayer [33,71]) the additional electrons fill up the states near the bottom of the conduction band at the K point at low temperatures, which leads to an efficient formation of trions and hinders neutral exciton formation due to Pauli blocking. As the temperature is raised, the Fermi-Dirac distribution smears out to higher energies and different momenta. This results in a reduction of low-energy excess carriers close to the K point. In turn, the number of optically bright trions within the light cone decreases, while the creation of neutral bright excitons is enhanced. Our results in Fig. 2(d) are consistent with this effect and confirm the assignment of T_{A1}^{1s} and T_{A2}^{1s} to the trions and X_A^{1s} to the neutral exciton. We note that the trion

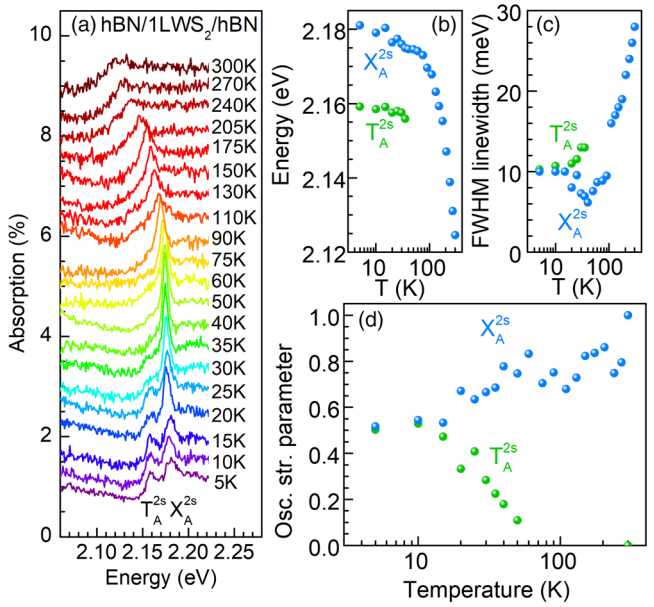

FIG. 3. (a) Absorption spectrum around the ($n = 2$) A exciton measured as a function of temperature ($T = 5$–300 K). The spectra are shifted along the $\boldsymbol{y}$ axis for clarity. The spectral line shapes are fitted as described in the text. The transition energies, FWHM linewidths, and oscillator strength parameters of the $2s$ trion T_A^{2s}, and the $2s$ exciton X_A^{2s} are plotted in (b),(c), and (d), respectively. Notably in (d), T_A^{2s} loses oscillator strength, while the X_A^{2s} gains strength, as the temperature is increased. This is trend is accompanied by an initial reduction of the X_A^{2s} linewidth shown in (c).

signature is negligibly small above $T = 110$ K, and is not analyzed using our model at these temperatures.

The temperature-dependent absorption around the spectral region of the $2s$ states is shown in Fig. 3(a). The extracted redshifts [Fig. 3(b)] are of similar size as observed for the $1s$ states and we refer to its discussion above. Furthermore, we find that the absorption amplitude of T_A^{2s} resonance decreases as temperature is increased, while X_A^{2s} gains strength [Fig. 3(d)]. This effect supports our assignment of a T-X pair to these two resonances. The transfer of oscillator strength is interestingly accompanied by the initial reduction of the linewidth of X_A^{2s} from $T = 5$ K up to 40 K, until T_A^{2s} disappears [Fig. 3(c)]. This observation may be consistently explained as follows. At low temperatures ($T = 5$ K), the T_A^{2s} has a similar oscillator strength as the X_A^{2s} and serves as a relaxation channel (T_A^{2s}) below X_A^{2s}, causing a relatively larger X_A^{2s} linewidth [1,65]. As the temperature is increased, the $2s$ trion states disappear. Therefore, the absence of initially available scattering states for the $2s$ excitons should lead to a reduction of the linewidth [65]. Even though such a mechanism should also be observable for the $X_A^{1s} - T_A^{1s}$ pair [see Fig. 2(c)], a significantly smaller (at least 1 order of magnitude) oscillator strength of T_A^{1s} in comparison to X_A^{1s} might conceal its observation.

In conclusion, we have discovered an excited bound three-particle state below the $2s$ neutral exciton in 1L WS_2 using optical absorption spectroscopy at different temperatures and GW-BSE calculations. A transfer of oscillator strength from the trions to neutral excitons with increasing temperature is established as an optical fingerprint of this T-X pair. Our work extends the knowledge of charged excitations and underlines their importance for the entire optical spectrum of doped 2D semiconductors.

The authors acknowledge financial support from the German Research Foundation (DFG Projects No. AR 1128/1-1, No. AR 1128/1-2 and No. DE 2749/2-1), and from the Villum Foundation. We gratefully acknowledge the computing time granted by the John von Neumann Institute for Computing and provided on the supercomputer JUWELS at Jülich Supercomputing Centre.

*arora@uni-muenster.de
†These authors contributed equally to this work.

[1] C. F. Klingshirn, *Semiconductor Optics* (Springer Berlin Heidelberg, Berlin, Heidelberg, 2012).
[2] M. A. Lampert, Phys. Rev. Lett. **1**, 450 (1958).
[3] G. A. Thomas and T. M. Rice, Solid State Commun. **23**, 359 (1977).
[4] T. Kawabata, K. Muro, and S. Narita, Solid State Commun. **23**, 267 (1977).
[5] B. Stebe, T. Sauder, M. Certier, and C. Comte, Solid State Commun. **26**, 637 (1978).
[6] B. Stébé and A. Ainane, Superlattices Microstruct. **5**, 545 (1989).
[7] K. Kheng, R. T. Cox, Merle Y. d' Aubigné, F. Bassani, K. Saminadayar, and S. Tatarenko, Phys. Rev. Lett. **71**, 1752 (1993).
[8] H. Buhmann, L. Mansouri, J. Wang, P. H. Beton, N. Mori, L. Eaves, M. Henini, and M. Potemski, Phys. Rev. B **51**, 7969 (1995).
[9] R. J. Warburton, C. S. Dürr, K. Karrai, J. P. Kotthaus, G. Medeiros-Ribeiro, and P. M. Petroff, Phys. Rev. Lett. **79**, 5282 (1997).
[10] R. Matsunaga, K. Matsuda, and Y. Kanemitsu, Phys. Rev. Lett. **106**, 037404 (2011).
[11] A. Chernikov, T. C. Berkelbach, H. M. Hill, A. Rigosi, Y. Li, O. B. Aslan, D. R. Reichman, M. S. Hybertsen, and T. F. Heinz, Phys. Rev. Lett. **113**, 076802 (2014).
[12] K. He, N. Kumar, L. Zhao, Z. Wang, K. F. Mak, H. Zhao, and J. Shan, Phys. Rev. Lett. **113**, 026803 (2014).
[13] G. Wang, A. Chernikov, M. M. Glazov, T. F. Heinz, X. Marie, T. Amand, and B. Urbaszek, Rev. Mod. Phys. **90**, 021001 (2018).
[14] K. F. Mak, K. He, C. Lee, G. H. Lee, J. Hone, T. F. Heinz, and J. Shan, Nat. Mater. **12**, 207 (2013).
[15] A. V. Stier, N. P. Wilson, K. A. Velizhanin, J. Kono, X. Xu, and S. A. Crooker, Phys. Rev. Lett. **120**, 057405 (2018).
[16] G. Plechinger, P. Nagler, J. Kraus, N. Paradiso, C. Strunk, C. Schüller, and T. Korn, Phys. Status Solidi **9**, 457 (2015).

[17] M. Barbone, A. R. P. Montblanch, D. M. Kara, C. Palacios-Berraquero, A. R. Cadore, D. De Fazio, B. Pingault, E. Mostaani, H. Li, B. Chen, K. Watanabe, T. Taniguchi, S. Tongay, G. Wang, A. C. Ferrari, and M. Atatüre, Nat. Commun. **9**, 3721 (2018).
[18] S.-Y. Chen, T. Goldstein, T. Taniguchi, K. Watanabe, and J. Yan, Nat. Commun. **9**, 3717 (2018).
[19] Z. Li, T. Wang, Z. Lu, C. Jin, Y. Chen, Y. Meng, Z. Lian, T. Taniguchi, K. Watanabe, S. Zhang, D. Smirnov, and S.-F. Shi, Nat. Commun. **9**, 3719 (2018).
[20] C. E. Stevens, J. Paul, T. Cox, P. K. Sahoo, H. R. Gutiérrez, V. Turkowski, D. Semenov, S. A. McGill, M. D. Kapetanakis, I. E. Perakis, D. J. Hilton, and D. Karaiskaj, Nat. Commun. **9**, 3720 (2018).
[21] Z. Ye, L. Waldecker, E. Y. Ma, D. Rhodes, A. Antony, B. Kim, X.-X. Zhang, M. Deng, Y. Jiang, Z. Lu, D. Smirnov, K. Watanabe, T. Taniguchi, J. Hone, and T. F. Heinz, Nat. Commun. **9**, 3718 (2018).
[22] D. Y. Qiu, F. H. da Jornada, and S. G. Louie, Phys. Rev. B **93**, 235435 (2016).
[23] D. Y. Qiu, F. H. da Jornada, and S. G. Louie, Phys. Rev. Lett. **111**, 216805 (2013).
[24] J. P. Echeverry, B. Urbaszek, T. Amand, X. Marie, and I. C. Gerber, Phys. Rev. B **93**, 121107(R) (2016).
[25] T. C. Berkelbach, M. S. Hybertsen, and D. R. Reichman, Phys. Rev. B **88**, 045318 (2013).
[26] A. Srivastava and A. Imamoğlu, Phys. Rev. Lett. **115**, 166802 (2015).
[27] J. Zhou, W.-Y. Shan, W. Yao, and D. Xiao, Phys. Rev. Lett. **115**, 166803 (2015).
[28] M. Trushin, M. O. Goerbig, and W. Belzig, Phys. Rev. B **94**, 041301(R), (2016).
[29] D. K. Efimkin and A. H. MacDonald, Phys. Rev. B **95**, 035417 (2017).
[30] P. Back, M. Sidler, O. Cotlet, A. Srivastava, N. Takemura, M. Kroner, and A. Imamoğlu, Phys. Rev. Lett. **118**, 237404 (2017).
[31] M. Sidler, P. Back, O. Cotlet, A. Srivastava, T. Fink, M. Kroner, E. Demler, and A. Imamoglu, Nat. Phys. **13**, 255 (2017).
[32] D. Van Tuan, M. Yang, and H. Dery, Phys. Rev. B **98**, 125308 (2018).
[33] T. Deilmann and K. S. Thygesen, Phys. Rev. B **96**, 201113(R) (2017).
[34] S.-Y. Shiau, M. Combescot, and Y.-C. Chang, Phys. Rev. B **86**, 115210 (2012).
[35] M. Drüppel, T. Deilmann, P. Krüger, and M. Rohlfing, Nat. Commun. **8**, 2117 (2017).
[36] B. Ganchev, N. Drummond, I. Aleiner, and V. Fal'ko, Phys. Rev. Lett. **114**, 107401 (2015).
[37] R. N. Hill, Phys. Rev. Lett. **38**, 643 (1977).
[38] See Supplemental Material at http://link.aps.org/supplemental/10.1103/PhysRevLett.123.167401 for details of the sample fabrication, experimental methods and spectral modeling, which includes Refs. [39–48], and for details on theoretical methods, which includes Refs. [22,49–54].
[39] A. Castellanos-Gomez, M. Buscema, R. Molenaar, V. Singh, L. Janssen, H. S. J. van der Zant, and G. A. Steele, 2D Mater. **1**, 011002 (2014).
[40] S. L. Chuang, *Physics of Optoelectronic Devices* (John Wiley and Sons, Inc., New York, 1995).
[41] N. Saigal, V. Sugunakar, and S. Ghosh, Appl. Phys. Lett. **108**, 132105 (2016).
[42] M. Koperski, M. R. Molas, A. Arora, K. Nogajewski, A. O. Slobodeniuk, C. Faugeras, and M. Potemski, Nanophotonics **6**, 1289 (2017).
[43] M. R. Molas, A. O. Slobodeniuk, K. Nogajewski, M. Bartos, Ł. Bala, A. Babiński, K. Watanabe, T. Taniguchi, C. Faugeras, and M. Potemski, Phys. Rev. Lett. **123**, 136801 (2019).
[44] R. J. Elliott, Phys. Rev. **108**, 1384 (1957).
[45] M. Shinada and S. Sugano, J. Phys. Soc. Jpn. **21**, 1936 (1966).
[46] A. Esser, R. Zimmermann, and E. Runge, Phys. Status Solidi **227**, 317 (2001).
[47] T. Deilmann and M. Rohlfing, Nano Lett. **17**, 6833 (2017).
[48] R. C. Miller, D. A. Kleinman, W. T. Tsang, and A. C. Gossard, Phys. Rev. B **24**, 1134 (1981).
[49] L. Hedin, Phys. Rev. **139**, A796 (1965).
[50] M. Rohlfing, Phys. Rev. B **82**, 205127 (2010).
[51] M. Drüppel, T. Deilmann, J. Noky, P. Marauhn, P. Krüger, and M. Rohlfing, Phys. Rev. B **98**, 155433 (2018).
[52] M. Rohlfing and S. G. Louie, Phys. Rev. B **62**, 4927 (2000).
[53] G. Onida, L. Reining, and A. Rubio, Rev. Mod. Phys. **74**, 601 (2002).
[54] T. Deilmann, M. Drüppel, and M. Rohlfing, Phys. Rev. Lett. **116**, 196804 (2016).
[55] F. Cadiz, E. Courtade, C. Robert, G. Wang, Y. Shen, H. Cai, T. Taniguchi, K. Watanabe, H. Carrere, D. Lagarde, M. Manca, T. Amand, P. Renucci, S. Tongay, X. Marie, and B. Urbaszek, Phys. Rev. X **7**, 021026 (2017).
[56] O. A. Ajayi, J. V Ardelean, G. D. Shepard, J. Wang, A. Antony, T. Taniguchi, K. Watanabe, T. F. Heinz, S. Strauf, X.-Y. Zhu, and J. C. Hone, 2D Mater. **4**, 031011 (2017).
[57] J. Wierzbowski, J. Klein, F. Sigger, C. Straubinger, M. Kremser, T. Taniguchi, K. Watanabe, U. Wurstbauer, A. W. Holleitner, M. Kaniber, K. Müller, and J. J. Finley, Sci. Rep. **7**, 12383 (2017).
[58] G. Plechinger, P. Nagler, A. Arora, R. Schmidt, A. Chernikov, A. Granados del Águila, P. C. M. Christianen, R. Bratschitsch, C. Schüller, and T. Korn, Nat. Commun. **7**, 12715 (2016).
[59] D. Van Tuan, B. Scharf, Z. Wang, J. Shan, K. F. Mak, I. Žutić, and H. Dery, Phys. Rev. B **99**, 085301 (2019).
[60] D. Vaclavkova, J. Wyzula, K. Nogajewski, M. Bartos, A. O. Slobodeniuk, C. Faugeras, M. Potemski, and M. R. Molas, Nanotechnology **29**, 325705 (2018).
[61] R. Schmidt, I. Niehues, R. Schneider, M. Drüppel, T. Deilmann, M. Rohlfing, S. M. de Vasconcellos, A. Castellanos-Gomez, and R. Bratschitsch, 2D Mater. **3**, 021011 (2016).
[62] D. Christiansen, M. Selig, G. Berghäuser, R. Schmidt, I. Niehues, R. Schneider, A. Arora, S. M. de Vasconcellos, R. Bratschitsch, E. Malic, and A. Knorr, Phys. Rev. Lett. **119**, 187402 (2017).
[63] A. Arora, M. Koperski, K. Nogajewski, J. Marcus, C. Faugeras, and M. Potemski, Nanoscale **7**, 10421 (2015).
[64] A. Arora, K. Nogajewski, M. Molas, M. Koperski, and M. Potemski, Nanoscale **7**, 20769 (2015).

[65] M. Selig, G. Berghäuser, A. Raja, P. Nagler, C. Schüller, T. F. Heinz, T. Korn, A. Chernikov, E. Malic, and A. Knorr, Nat. Commun. **7**, 13279 (2016).

[66] S. Shree, M. Semina, C. Robert, B. Han, T. Amand, A. Balocchi, M. Manca, E. Courtade, X. Marie, T. Taniguchi, K. Watanabe, M. M. Glazov, and B. Urbaszek, Phys. Rev. B **98**, 035302 (2018).

[67] W. Zhao, R. M. Ribeiro, M. Toh, A. Carvalho, C. Kloc, A. H. Castro Neto, and G. Eda, Nano Lett. **13**, 5627 (2013).

[68] G. V Astakhov, V. P. Kochereshko, D. R. Yakovlev, W. Ossau, J. Nürnberger, W. Faschinger, and G. Landwehr, Phys. Rev. B **62**, 10345 (2000).

[69] V. Ciulin, P. Kossacki, S. Haacke, J.-D. Ganière, B. Deveaud, A. Esser, M. Kutrowski, and T. Wojtowicz, Phys. Rev. B **62**, R16310 (2000).

[70] R. A. Suris, V. P. Kochereshko, G. V. Astakhov, D. R. Yakovlev, W. Ossau, J. Nürnberger, W. Faschinger, G. Landwehr, T. Wojtowicz, G. Karczewski, and J. Kossut, Phys. Status Solidi **227**, 343 (2001).

[71] E. Courtade, M. Semina, M. Manca, M. M. Glazov, C. Robert, F. Cadiz, G. Wang, T. Taniguchi, K. Watanabe, M. Pierre, W. Escoffier, E. L. Ivchenko, P. Renucci, X. Marie, T. Amand, and B. Urbaszek, Phys. Rev. B **96**, 085302 (2017).